Divalent Ytterbium Boratabenzene Complex $(C_5H_5BNPh_2)_2Yb(THF)_2$: Synthesis, Structure, and Solvent-Mediated Redox Transformation

Peng Cui, Yaofeng Chen,* Guoping Wang,‡ Guangyu Li, and Wei Xia

State Key Laboratory of Organometallic Chemistry, Shanghai Institute of Organic Chemistry, Chinese Academy of Science, 354 Fenglin Road, Shanghai 200032, People's Republic of China, and Department of Chemistry, Zhejiang University, Hangzhou 310027, People's Republic of China

Received March 16, 2008

*Summary: The boratabenzene derivative of divalent ytterbium complex $(C_5H_5BNPh_2)_2Yb(THF)_2$ (**1**) was synthesized and characterized. Reaction of* **1** *with α-diimine PhNC(Me)C(Me)NPh in toluene afforded a trivalent ytterbium complex, $[C_5H_5BNPh_2]_2Yb[PhNC(Me)C(Me)NPh]$ (**2**), which was characterized by single-crystal X-ray diffraction. The redox process is solvent sensitive and reversible.*

Introduction

Divalent lanthanide complexes have fantastic reductive properties.[1] Due to α-diimine ligands' versatile coordination modes and interesting redox properties, the redox reactions of the divalent lanthanide complexes with α-diimine ligands have received increasing attention with respect to investigation of intramolecular metal−ligand electron transfer.[2] The ytterbium complexes are the ideal candidates for this purpose by virtue of a low Yb(II)/Yb(III) transformation potential.[3] Furthermore, the Yb(II)/Yb(III) systems, which undergo facile and reversible redox transformations by intramolecular electronic transfer, are of potential interest for the construction of molecular switches.[2b] The redox reactions of divalent ytterbocenes with α-diimine ligands have been extensively studied and are greatly influenced by the types of divalent ytterbocenes and α-diimine ligands involved. A variety of new organometallic complexes were produced, some of which displayed unusual structural features or interesting properties.[2b,4]

Boratabenzenes are heterocyclic, 6π-electron, aromatic anions that have been introduced into organometallic chemistry as counterparts of Cp ligands with poorer electron-donating properties.[5] Recent reports have described an increasing number of organometallic complexes of transition metals bearing boratabenzenes.[6] On the other hand, examples of boratabenzene derivatives of lanthanides are very rare, and their reactivities remain little explored.[7,8] Previously we reported the divalent samarium borotabenzene complexes and their catalytic behaviors toward methyl methacrylate polymerization.[9] To further explore the chemistry of the boratabenzene derivatives of divalent lanthanides, we prepared the first divalent ytterbium borotabenzene complex and studied its redox transformation with α-diimine ligands.

Scheme 1

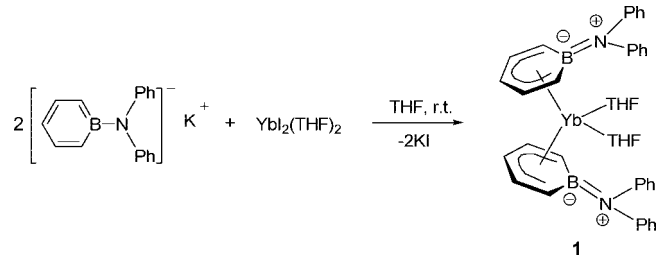

1

Results and Discussion

Synthesis and Characterization of $(C_5H_5BNPh_2)_2Yb(THF)_2$(1). Ligand salt $[C_5H_5BN(C_6H_5)_2]^-K^+$ was prepared by Fu's method.[10] Subsequent salt elimination with $YbI_2(THF)_2$ in THF at room temperature provided the target divalent ytterbium boratabenzene complex **1** as dark red, blocky crystals in 54% yield (Scheme 1). Complex **1** is readily soluble in THF, less soluble in benzene, and sensitive to air and moisture. The solution NMR spectroscopy of **1** showed the complex is diamagnetic, consistent with the Yb(II) oxidation state. The elemental analysis and ^1H NMR spectroscopy of **1** in C_6D_6 indicated that one Yb(II) ion was

* To whom correspondence should be addressed. E-mail: yaofchen@mail.sioc.ac.cn. Fax: (+86)2164166128.

‡ To whom correspondence concerning the magnetic moment and ESR studies for complex **2** should be addressed.

(1) (a) Evans, W. J. *Coord. Chem. Rev.* **2000**, *206−207*, 263. (b) Evans, W. J. *Inorg. Chem.* **2007**, *46*, 3435.

(2) (a) Bochkarev, M. N.; Trifonov, A. A.; Cloke, F. G. N.; Dalby, C. I.; Matsunaga, P. T.; Andersen, R. A.; Schumann, H.; Loebel, J.; Hemling, H. *J. Organomet. Chem.* **1995**, *486*, 177. (b) Trifonov, A. A. *Eur. J. Inorg. Chem.* **2007**, 3151. (c) Walter, M. D.; Berg, D. J.; Andersen, R. A. *Organometallics.* **2007**, *26*, 2296. (d) Moore, J. A.; Cowley, A. H.; Gordon, J. C. *Organometallics.* **2006**, *25*, 5207.

(3) General reduction potentials of Ln(III)/Ln(II) vs NHE: Eu (−0.35 V), Yb (−1.15 V), Sm (−1.55 V), Tm (−2.3 V), Nd (−2.6 V), Dy (−2.6 V), Pr (−2.7 V) and La (−3.1 V). See ref 1a and references therein.

(4) (a) Trifonov, A. A.; Fedorova, E. A.; Fukin, G. K.; Druzhkov, N. O.; Bochkarev, M. N. *Angew. Chem., Int. Ed.* **2004**, *43*, 5045. (b) Trifonov, A. A.; Borovkov, I. A.; Fedorova, E. A.; Fukin, G. K.; Larionova, J.; Druzhkov, N. O.; Cherkasov, V. K. *Chem.−Eur. J.* **2007**, *13*, 4981. (c) Trifonov, A. A.; Fedorova, E. A.; Ikorskii, V. N.; Dechert, S.; Schumann, H.; Bochkarev, M. N. *Eur. J. Inorg. Chem.* **2005**, 2812.

(5) Herberich, G. E.; Holger, O. *Adv. Organomet. Chem.* **1986**, *25*, 199.

(6) (a) Ashe, A. J., III; Al-Ahmad, S.; Fang, X. G. *J. Organomet. Chem.* **1999**, *581*, 92. (b) Fu, G. C. *Adv. Organomet. Chem.* **2001**, *47*, 101. (c) Bazan, G. C.; Rodriguez, G.; Ashe, A. J., III; Al-Ahmad, S.; Müller, C. *J. Am. Chem. Soc.* **1996**, *118*, 2291. (d) Rogers, J. S.; Bu, X. H.; Bazan, G. C. *J. Am. Chem. Soc.* **2000**, *122*, 730. (e) Ashe, A. J., III; Al-Ahmad, S.; Fang, X. D.; Kampf, J. W. *Organometallics* **2001**, *20*, 468. (f) Herberich, G. E.; Basu Baul, T. S.; Englert, U. *Eur. J. Inorg. Chem.* **2002**, 43. (g) Auvray, N.; Basu Baul, T. S.; Braunstein, P.; Croizat, P.; Englert, U.; Herberich, G. E.; Welter, R. *Dalton Trans.* **2006**, 2950.

(7) For the reported boratabenzene lanthanide metal complexes, see: Wang, B.; Zheng, X. L.; Herberich, G. E. *Eur. J. Inorg. Chem.* **2002**, 31.

(8) For the reported boratabenzene Y and Sc complexes, see: (a) Zheng, X. L.; Wang, B.; Englert, U.; Herberich, G. E. *Inorg. Chem.* **2001**, *40*, 3117. (b) Herberich, G. E.; Englert, U.; Fischer, A.; Ni, J. H.; Schmitz, A. *Organometallics* **1999**, *18*, 5496. (c) Putzer, M. A.; Rogers, J.; Bazan, G. *J. Am. Chem. Soc.* **1999**, *121*, 8112.

(9) Cui, P.; Chen, Y. F.; Zeng, X, H.; Sun, J.; Li, G. Y.; Xia, W. *Organometallics* **2007**, *26*, 6519.

(10) Hoic, D. A.; DiMare, M.; Fu, G. C. *J. Am. Chem. Soc.* **1997**, *119*, 7155.

10.1021/om800245u CCC: $40.75
Publication on Web 06/25/2008

Chart 1

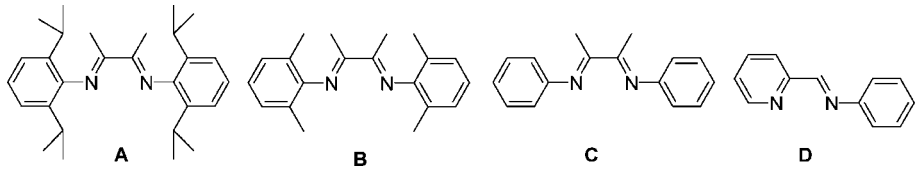

ligated by two boratabenzene ligands (^{1}H NMR (C_6D_6): δ 7.18, 6.29, and 6.01 ppm for *m*-H, *o*-H, and *p*-H on the boratabenzene ring) and two THF molecules (^{1}H NMR (C_6D_6): δ 3.35 and 1.14 ppm).

Single crystals of complex **1** were obtained by diffusion of hexane into a THF solution and characterized by X-ray diffraction. An ORTEP diagram is shown in Figure 1. Complex **1** exhibits a bent metallocene-type structure wherein the NPh_2 groups point away from the metallocene wedge and the Yb center adopts a pseudotetrahedral geometry. The Yb−C bond lengths are significantly longer for B1 (2.966 Å) and C1 (2.880 Å) vs C2 (2.845 Å), C3 (2.779 Å), C4 (2.796 Å), and C5 (2.849 Å), which reveals a slippage of Yb away from B and toward C3 to give an intermediate (η^4−η^6) coordination mode as observed in other transition metal boratabenzene complexes.[5] The average Yb−C distance in **1** is 2.83 Å, which is significantly longer than those in the related Cp complexes, such as $(C_5H_4PPh_2)_2Yb(DME)$ (2.71 Å),[11] $(C_5H_4SiMe_3)_2Yb(THF)_2$ (2.75 Å),[12] and $(C_5Me_5)_2Yb(THF)(NH_3)$ (2.78 Å).[13] The longer Yb−C distances in **1** are consistent with the weaker donor properties of the boratabenzene ligands compared to the Cp-type ligands. The trigonal planar geometry around the nitrogen atom (∠B1−N1−C6 = 123.7°, ∠B1−N1−C12 = 120.6°, ∠C6−N1−C12 = 115.7°; ∑ = 360°) and the rather short B1−N1 bond distance of 1.480(10) Å indicate a fairly strong π-interaction between boron and the NPh_2 moiety.[10]

Reactions of 1 with α-Diimines and Characterization of $[C_5H_5BNPh_2]_2Yb[PhNC(Me)C(Me)NPh]$ (2). Four α-diimines, *N*,*N*′-bis(2,6-diisopropylphenyl)-1,2-bis(methyl)ethanediimine (**A**), *N*,*N*′-bis(2,6-dimethylphenyl)-1,2-bis(methyl)ethanediimine (**B**), *N*,*N*′-bis(phenyl)-1,2-bis(methyl)ethanediimine (**C**), and *N*-(2-pyridylmethylene)benzeneamine (**D**) (Chart 1) were synthesized according to the literature.[14] Reactions of **1** with these four α-diimines were studied. The addition of 1 equiv of **A** or **B** to the dark red toluene solution of **1** did not change the color of the solution, even when the reaction mixtures were stirred at 60 °C overnight. The solvent was removed in vacuo, and the ^{1}H NMR spectroscopy of the dark red residues in C_6D_6 showed that no reaction had occurred between **1** and **A** or **B**. However, a quick color change of the solution from red to dark green was observed when **C** or **D** was added to **1** in toluene. The difference in reactivities of diimines to **1** can be ascribed to the steric effect, and the diimines with less bulky substitutents usually are more reactive.[2b]

The reaction between **1** and α-diimine **C** was studied in detail. The addition of 1 equiv of **C** to **1** in toluene at room temperature gave a deep green reaction mixture, which when cooled to −35 °C provided a new complex as deep green crystals. The new complex is slightly soluble in benzene and sensitive to air and moisture. ^{1}H NMR spectroscopy of the complex in C_6D_6 showed a paramagnetic property. The phenyl and methyl groups of the diimine displayed four peaks at 38.03, −27.66, −39.16, and 0.30 ppm, respectively, and signals for protons on the boratabenzene ligand appeared in the range from 6 to 15 ppm. The ratio of diimine to boratabenzene ligand is 1:2.

Single crystals of the new complex were grown from a solution mixture of toluene and hexane, and the solid-state structure was determined by crystallographic methods (Figure 2). The complex is therefore **2**, as shown in Scheme 2. The ytterbium center has a pseudotetrahedral geometry with two boratabenzene ligands and one diimine ligand bound through two nitrogen atoms. The orientation of the NPh_2 groups in **2** is completely different from that in **1**: one NPh_2 group points toward the metallocene wedge, while the other is rotated to the opposite position. The Yb−$Ring_{(cent.)}$ distances in **2** (2.407 and 2.408 Å) are 0.06 Å shorter than that in **1** (2.469 Å), indicating a Yb oxidation state change from Yb(II) in **1** into Yb(III) in **2**. As observed in other Yb(II) →Yb(III) systems, the difference in Yb−$Ring_{(cent.)}$ distances between **1** and **2** is less than the ionic radii difference between Yb(II) and Yb(III) (0.155 Å), which can be attributed to the steric crowding in **2**.[2b] The structural data (B1−N1 = 1.475 Å, ∠B1−N1−C6 = 126.1°, ∠B1−N1−C12 = 117.4°, ∠C6−N1−C12 = 116.1°, ∑ = 359.6°; B2−N2 = 1.506 Å, ∠B2−N2−C23 = 125.3°, ∠B2−N2−C29 = 119.3°, ∠C23−N2−C29 = 115.3°, ∑ = 359.9°) showed the strong B−N π-interaction is retained in **2**.

The coordination pattern of the α-diimine fragment to the Yb ion in **2** is very special. The related Cp complexes usually exhibited two equal Yb−N bonds and a delocalized NCCN π-system.[2b,c] In **2**, the Yb−N4 bond length (2.391 Å) fell in the range 2.306−2.394 Å observed for the related Cp complexes;

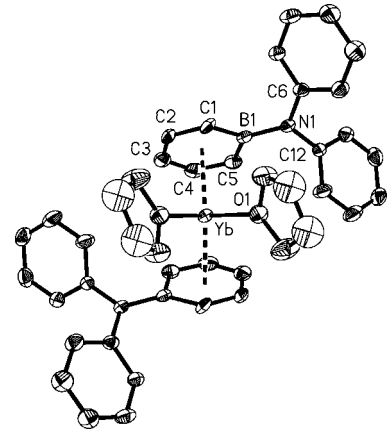

Figure 1. Molecular structure of **1** with thermal ellipsoids at the 30% probability level. Selected bond distances (Å) and angles (deg): Yb−B1 = 2.966(7), Yb−C1 = 2.880(9), Yb−C2 = 2.845(7), Yb−C3 = 2.779(7), Yb−C4 = 2.796(8), Yb−C5 = 2.849(7), Yb−Ring(cent.)= 2.469, Yb−O1 = 2.461(5), B1−N1 = 1.480(10), ∠O1−Yb−O1A = 76.4(3), ∠B1−N1−C6 = 123.7(6), ∠B1−N1−C12 = 120.6(6), ∠C6−N1−C12 = 115.7(6), ∠Ring(cent.)−Yb−Ring(cent.) = 128.8.

(11) Lin, G. Y.; Wong, W. T. *J. Organomet. Chem.* **1995**, *495*, 203.
(12) Lappert, M. F.; Yarrow, P. I. W.; Atwood, J. L.; Shakir, R.; Holton, J. *J. Chem. Soc. Chem. Commun.* **1980**, 987.
(13) Wayda, A. L.; Dye, J. L.; Rogers, R. D. *Organometallics.* **1984**, *3*, 1605.
(14) (a) Lemp, E.; Zanocco, A. L.; Günther, G.; Pizarro, N. *Tetrahedron* **2006**, *62*, 10734. (b) Türkmen, H.; Çetinkaya, B. *J. Organomet. Chem.* **2006**, *691*, 3749.

Scheme 2

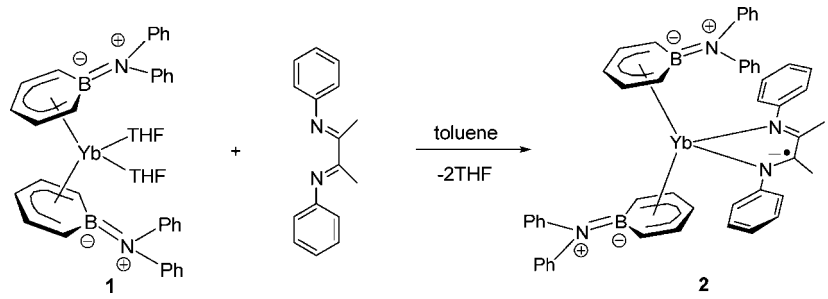

however, the Yb−N3 bond length (2.451 Å) is significant longer. The Yb−N bond length difference (0.06 Å) in **2** is very close to that found in Yb(η^5-$C_{13}H_9$)[(2,6-^{i}Pr$_2$)C_6H_3-N=C(−CH_3)-C(=CH_2)-*N*-(2,6-^{i}Pr$_2$)C_6H_3](THF) (0.07 Å), in which one nitrogen atom acts as a neutral donor and the other as an anionic donor.[4a] Consistent with the nonequivalent Yb−N bonds, the C35−N3 distance (1.300 Å) is shorter than the C36−N4 distance (1.332 Å). In addition, the C35−C36 distance (1.464 Å) is nearly the same as that in the neutral α-diimine ^{t}Bu-N=CH-CH=N-^{t}Bu (1.467 Å).[15] Therefore, the solid-state structure of **2** is better depicted as that in Scheme 2; the NCCN unit is localized or partly delocalized. The nonequivalent bonding situation in **2** is probably due to the different donating ability of the atoms on the boratabenzene ring.

The magnetic moments for **2** in the solid state were measured; the field dependence of the magnetization at 300 K is illustrated in Figure 3. The magnetic moment values for **2** increased regularly with the magnetic field strength in the magnetic field of 0 to 3 kOe, this positive magnetic susceptibility is consistent with the paramagnetic property as observed in the solution NMR spectrum. However, the magnetic susceptibility of **2** becomes negative in the magnetic field of 3 to 10 kOe, which reveals a weak diamagnetic behavior. The reason for this phenomenon is unknown at this stage. The ESR investigation of **2** was also carried out at 300 K, and no signal was observed.

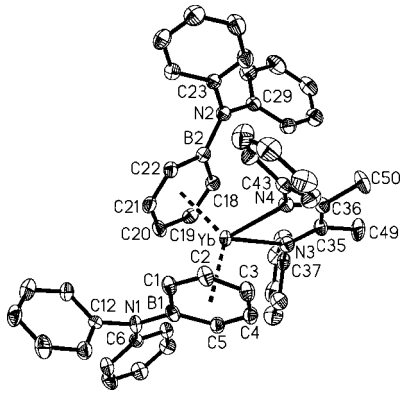

Figure 2. Molecular structure of **2** with thermal ellipsoids at the 30% probability level. Selected bond distances (Å) and angles (deg): Yb−B1 = 2.960(6), Yb−C1 = 2.835(7), Yb−C2 = 2.758(7), Yb−C3 = 2.707(8), Yb−C4 = 2.720(8), Yb−C5 = 2.800(7), Yb−B2 = 2.997(7), Yb−C18 = 2.832(7), Yb−C19 = 2.724(7), Yb−C20 =2.681(7), Yb−C21 = 2.724(7), Yb−C22 = 2.835(7), B1−N1 = 1.475(10), B2−N2 = 1.506(11) Yb−N3 = 2.451(6), Yb−N4 = 2.391(6), N3−C35 = 1.300(9), N4−C36 = 1.332(9), C35−C49 = 1.504(10), C35−C36 = 1.464(10), C36−C50 = 1.498(10), Yb−Ring(cent.) = 2.407 and 2.408, ∠N3−Yb−N4 = 66.13(19), ∠B1−N1−C6 = 126.1(6), ∠B1−N1−C12=117.4(6),∠C6−N1−C12=116.1(6),∠B2−N2−C23 = 125.3(6), ∠B2−N2−C29 = 119.3(6), ∠C23−N2−C29 = 115.3(6), ∠Ring(cent.)−Yb−Ring(cent.) = 130.7.

During the study on the reaction of **1** with α-diimine **C**, it was observed that no reaction occurred while THF was used as the solvent. Therefore, it is interesting to check if **2** is stable in THF. The dark green **2** was dissolved in THF-d_8, which gave a dark red solution immediately, and the ^{1}H NMR spectroscopy showed the disappearance of **2** and the formation of free α-diimine **C** (^{1}H NMR (THF-d_8): δ 2.12 ppm for −CH_3, 6.77 and 7.08 ppm for ph-H^2 and ph-H^4; signals for ph-H^3 are overlapped with those for the protons of the boratabenzene ligand) and the diamagnetic divalent complex **1** (^{1}H NMR (THF-d_8): δ 5.96 and 6.14 ppm for *p*-H and *o*-H on the boratabenzene ring). The signals are broad with paramagnetism in the first few hours and finally change into sharp signals with normal coupling constants after 8 h. This result indicated that the displacement of the radical-anionic α-diimine **C** by THF-d_8 solvent molecules and an accompanying one-electron transfer from the radical-anionic α-diimine back to the Yb ion center. The foregoing observation revealed that the interaction between the radical-anionic α-diimine and the Yb ion is weak, which is also evidenced by the longer Yb−N distances in the solid-state structure of **2** in comparison to those of the Cp analogues. Similar solvent-mediated reversible redox transformations have been reported for other Yb α-diimine complexes.[2b] The reaction between **C** and **1**'s analogue, [$C_5H_5BN(C_6H_5)_2$]$_2$Sm(THF)$_2$ (**3**), has also been checked. The addition of 1 equiv of **C** to black **3** in C_6D_6 instantaneously gave a brown-red solution, and the ^{1}H NMR spectroscopy showed the disappearance of **3** and the formation of a new paramagnetic complex, which displayed a similar chemical shift pattern to that of the trivalent ytterbium complex [$C_5H_5BNPh_2$]$_2$Yb[PhNC(Me)C(Me)NPh] (**2**). Removal of the C_6D_6 solution in vacuo, followed by redissolution of the brown-red solid residue in THF-d_8 did not restore the divalent samarium complex **3**. This experiment indicated that, in contrast to that of **1**, the redox reaction of **3** with α-diimine **C** is not a solvent-mediated reversible process, due to a higher Sm(II)/Sm(III) transformation potential.

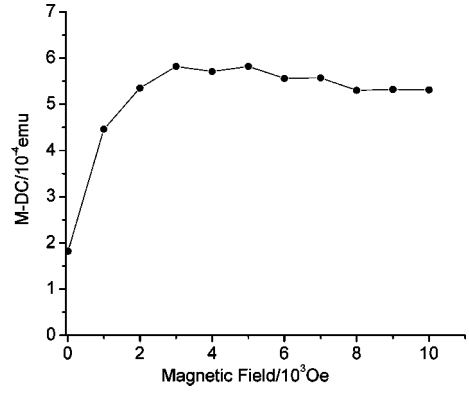

Figure 3. Field dependence of magnetization for **2** at 300 K.

Conclusions

In summary, the reaction of $[C_5H_5BN(C_6H_5)_2]^-K^+$ with $YbI_2(THF)_2$ provided the divalent ytterbium boratabenzene complex $(C_5H_5BNPh_2)_2Yb(THF)_2$ (**1**). The redox reactions of **1** with α-diimine ligands were greatly influenced by the steric circumstance in the α-diimines, and the reaction occurred only with the less bulky α-diimines. The redox reaction of **1** with α-diimine PhNC(Me)C(Me)NPh (**C**) in toluene afforded the trivalent ytterbium complex $[C_5H_5BNPh_2]_2Yb[PhNC(Me)C(Me)NPh]$ (**2**), in which the interaction between the radical-anionic α-diimine and the Yb ion is weak, and the redox process is solvent sensitive and reversible.

Experimental Section

General Procedures. All operations were carried out under an atmosphere of argon using standard Schlenk techniques or in a nitrogen-filled glovebox. THF was distilled from Na-benzophenone ketyl, and toluene and hexane were dried over Na/K alloy. C_6D_6 and THF-d_8 were dried over Na/K alloy, distilled under vacuum, and stored in the glovebox. $YbI_2(THF)_2$ was prepared from excess metal Yb and diiodomethane in THF according to the standard procedure.[16] $K[C_5H_5BN(C_6H_5)_2]$ was prepared by the method reported by Fu.[10] α-Diimine ligands were synthesized following the literature.[14] ^1H and ^{13}C NMR spectra were recorded on a Varian Mecury 300 MHz spectrometer at 300 and 75 MHz, respectively. ^{11}B NMR spectra were recorded on a Bruker DXP 400 MHz spectrometer at 128 MHz. All chemical shifts were reported in δ units with references to the residual solvent resonance of the deuterated solvents for proton and carbon chemical shifts, and to external $BF_3 \cdot OEt_2$ for boron chemical shifts. Infrared spectra were recorded on a Perkin-Elmer 983 spectrometer. The magnetic susceptibility data were collected by using a Quantum Design PPMS-9 magnetometer in the magnetic field of 0 to 10 kOe at 300 K under an argon atmosphere. The ESR spectrum was measured at X-band on a Bruker ESR300 instrument. Elemental analysis was performed by Analytical Laboratory of Shanghai Institute of Organic Chemistry. Melting points of the complexes were determined on a SWG X-4 digital melting point apparatus in a sealed capillary and are uncorrected.

$(C_5H_5BNPh_2)_2Yb(THF)_2$ (1). $YbI_2(THF)_2$ (520 mg, 1.048 mmol) and $K[C_5H_5BN(C_6H_5)_2]$ (586 mg, 2.096 mmol) were mixed in 25 mL of THF, and the reaction mixture was stirred overnight at room temperature. The solvent was removed under vacuum, and the dark red solid residue was extracted with 18 mL of toluene. Evaporation of the dark red extract solution in vacuo gave a dark red solid. The solid was washed with hexane and then dissolved in 4 mL of THF; 5 mL of hexane was layered to give dark red, blocky crystals (460 mg, 54% yield), mp 167−169 °C without decomposition. Anal. Calcd for $C_{42}H_{46}B_2N_2O_2Yb$: C, 62.63; H, 5.76; N, 3.48. Found: C, 61.86; H, 5.70; N, 3.69. ^1H NMR (300 MHz, C_6D_6, 25 °C): δ 7.29 (d, J = 7.8 Hz, 8H, NCC*H*CHCH), 7.20−7.11 (m, 12H, BCHC*H*CH, NCCHC*H*CH), 6.89 (t, J = 7.2 Hz, 4H, NCCHCHC*H*), 6.29 (d, J = 10.2 Hz, 4H, BC*H*CHCH), 6.01 (t, J = 6.9 Hz, 2H, BCHCHC*H*), 3.35 (br s, 8H, OCH_2CH$_2$), 1.14 (br s, 8H, OCH$_2$CH_2). ^1H NMR (300 MHz, THF-d_8, 25 °C): δ 7.17−7.06 (m, 20H, NCC*H*CHCH, BCHC*H*CH, NCCHC*H*CH), 6.87 (t, J = 6.8 Hz, 4H, NCCHCHC*H*), 6.03 (d, J = 10.2 Hz, 4H, BC*H*CHCH), 5.93 (t, J = 6.6 Hz, 2H, BCHCHC*H*), 3.61 (m, 8H, OCH_2CH$_2$), 1.77 (m, 8H, OCH$_2$CH_2). ^{13}C NMR (75 MHz, THF-d_8, 25 °C): δ 152.5, 136.9, 129.2, 126.8, 122.2, 117.5, 104.2, 68.2, 26.4. ^{11}B NMR (128 MHz, THF-d_8, 25 °C): δ 33.8. IR (KBr pellet, cm^{-1}): 3079, 3042, 3011, 2868, 1594, 1509, 1493, 1459, 1419, 1386, 1310, 1263, 1245, 1173, 1156, 1073, 1028, 996, 876, 748, 691.

$(C_5H_5BNPh_2)_2Yb[PhNC(Me)C(Me)NPh]$ (2). A toluene solution of α-diimine PhNC(Me)C(Me)NPh (20.5 mg, 0.087 mmol in 2 mL of toluene) was added to **1** (70 mg, 0.087 mmol) in 6 mL of toluene. The color of the solution immediately changed from dark red into dark green. After standing at room temperature overnight, the reaction mixture was cooled to −35 °C to give green crystals (44 mg, 56% yield), mp 244−246 °C without decomposition. Anal. Calcd for $C_{50}H_{46}B_2N_4Yb$: C, 66.91; H, 5.17; N, 6.24. Found: C, 66.28; H, 5.70; N, 6.26. **2** is paramagnetic. ^1H NMR (300 MHz, C_6D_6, 25 °C): δ 38.03 (s, 4H), 14.52(s, 4H), 13.67 (t, J = 7.2 Hz, 2H), 10.32 (s, 4H), 7.66 (t, J = 7.4 Hz, 8H), 7.48(t, J = 7.4 Hz, 4H), 6.48(d, J = 7.5 Hz, 8H), 0.30 (s, 6H), −27.66 (br s, 2H), −39.16(br s, 4H). ^{11}B NMR (128 MHz, C_6D_6, 25 °C): δ 1.8. IR (KBr pellet, cm^{-1}): 3083, 3065, 3056, 3046, 3017, 2965, 1633, 1592, 1494, 1456, 1417, 1384, 1355, 1310, 1244, 1207, 1170, 1153, 1117, 1072, 1021, 876, 808, 761, 747, 694.

Reaction of $(C_5H_5BNPh_2)_2Sm(THF)_2$with PhNC(Me)C(Me)NPh. The addition of PhNC(Me)C(Me)NPh (5 mg, 0.021 mmol) to $(C_5H_5BNPh_2)_2Sm(THF)_2$ (16.5 mg, 0.021 mmol) in 0.6 mL of C_6D_6 instantaneously gave a brown-red solution. After 10 min, a ^1H NMR spectroscopy was recorded. ^1H NMR (300 MHz, C_6D_6, 25 °C): δ 37.41 (s, 4H), 12.86 (s, 4H), 11.03 (d, J = 10.5 Hz, 4H), 9.09 (s, 2H), 8.40 (d, J = 6.9 Hz, 8H), 7.47 (t, J = 7.2 Hz, 8H), 6.99 (t, J = 7.3 Hz, 4H), 3.56 (m, 8H), 1.41 (m, 8H), −48.02 (s, 2H), −60.28 (s, 4H). The signals for two methyl groups on the α-diimine ligand were not observed.

X-ray Crystallography. Suitable single crystals of **1** and **2** were sealed in thin-walled glass capillaries, and data collection was performed at 20 °C on a Bruker SMART diffractometer with graphite-monochromated Mo Kα radiation (λ = 0.71073 Å). The SMART program package was used to determine the unit-cell parameters. The absorption correction was applied using SADABS. The structures were solved by direct methods and refined on F^2 by full-matrix least-squares techniques with anisotropic thermal parameters for non-hydrogen atoms. Hydrogen atoms were placed at calculated positions and were included in the structure calculation without further refinement of the parameters. All calculations were carried out using the SHELXS-97 program. Crystal data for **1**: $C_{42}H_{46}B_2N_2O_2Yb$, M_r = 805.47, T = 293(2) K, monoclinic, $C2/c$, a = 12.0930(12) Å, b = 13.7092(12) Å, c = 23.173(2) Å, β = 104.875(2)°, V = 3712.9(6) Å^3, Z = 4, 9856 reflections collected, 3653 independent reflections, R1 = 0.0663, wR2 = 0.1779 ($I > 2\sigma(I)$); **2**: $C_{50}H_{46}B_2N_4Yb$, M_r = 897.57, T = 293(2) K, triclinic, $P1$, a = 10.8679(17) Å, b = 13.486(2) Å, c = 14.778(2) Å, α = 100.474(3)°, β = 97.923(2)°, γ = 95.890(3)°, V = 2091.3(6) Å^3, Z = 2, 11 836 reflections collected, 8799 independent reflections, R1 = 0.0596, wR2 = 0.1301 ($I > 2\sigma(I)$).

Acknowledgment. This work was supported by the National Natural Science Foundation of China (Grant No. 20672134) and Chinese Academy of Science. We thank Prof. Changtao Qian (Shanghai Institute of Organic Chemistry) for helpful discussions.

Supporting Information Available: CIF files giving X-ray crystallographic data for **1** and **2** are available free of charge via the Internet at http://pubs.acs.org.

OM800245U

(15) Huige, C. J. M.; Spek, A. L.; de Boer, J. L. *Acta Crystallogr.* **1983**, *C41*, 113.

(16) Girard, P.; Namy, J. L.; Kagan, H. B. *J. Am. Chem. Soc.* **1980**, *102*, 2693.